A One-Class Variational Autoencoder (OCVAE) Cascade for Classifying Atypical Bone Marrow Cell Sub-types

Jonathan Tarquino[1,2], Jhonathan Rodriguez[1,2], Charlems Alvarez-Jimenez[1,2], and Eduardo Romero[1,2(✉)]

[1] Universidad Nacional de Colombia, Bogotá, Colombia
[2] Computer Imaging and Medical Applications Laboratory-CIM@LAB, Bogotá, Colombia
edromero@unal.edu.co
http://cimalab.unal.edu.co/

Abstract. Atypical bone marrow (BM) cell-subtype characterization defines the diagnosis and follow up of different hematologic disorders. However, this process is basically a visual task, which is prone to inter- and intra-observer variability. The presented work introduces a new application of one-class variational autoencoders (OCVAE) for automatically classifying the 4 most common pathological atypical BM cell-subtypes, namely myelocytes, blasts, promyelocytes, and erythroblasts, regardless the disease they are associated with. The presented OCVAE-based representation is obtained by concatenating the bottleneck of 4 separated OCVAEs, specifically set to capture one-cell-sub-type pattern at a time. In addition, this strategy provides a complete validation scheme in a subset of an open access image dataset, demonstrating low requirements in terms of number of training images. Each particular OCVAE is trained to provide specific latent space parameters (64 means and 64 variances) for the corresponding atypical cell class. Afterwards, the obtained concatenated representation space feeds different classifiers which discriminate the proposed classes. Evaluation is done by using a subset ($n = 26,000$) of a public single-cell BM image database, including two independent partitions, one for setting the VAEs to extract features ($n = 20,800$), and one for training and testing a set classifiers ($n = 5,200$). Reported performance metrics show the concatenated-OCVAE characterization successfully differentiates the proposed atypical BM cell classes with accuracy = 0.938, precision = 0.935, recall = 0.935, f1-score = 0.932, outperforming previously published strategies for the same task (handcrafted features, ResNext, ResNet-50, XCeption, CoAtnet), while a more thorough experimental validation is included.

Keywords: One-class Variational autoencoder · Atypical bone marrow cell · artificial intelligence · cytology imaging · automatic classification

H. Greenspan et al. (Eds.): MICCAI 2023, LNCS 14225, pp. 725–734, 2023.
https://doi.org/10.1007/978-3-031-43987-2_70

1 Introduction

Bone marrow (BM) lineage classification and differential counting are at the very base of most diagnoses or clinical management of hematopoietic disorders [7]. Despite advances in cytogenetics, immunophenotyping and molecular technology, morphology of BM cellular lineages is still the gold standard in hematology. This cell morphometry estimation is performed by highly trained and experienced proffesionals and yet, this activity has been reported with high intra- and inter-operator variability [10,13], and even more variable when visually identifying atypical BM cells [11,32]. This examination not only defines the stage of proliferating disorders, but also it characterizes chronic diseases associated with particular distributions of leukocyte sub-types or atypical BM cells [7]. On the one hand cell morphological examination is fully dependent on the operator experience-skills and, on the other hand not objective quantitative measurements are available [1].

In order to provide a more quantitative BM cell characterization, different strategies have been proposed, either extracting hand-crafted features or applying deep learning based approaches. Importantly, most of them has been focused on leukemia detection [3,25], which narrows application of automated strategies to a single hematological disease. Regarding classic machine learning approaches using hand-crafted features, different representation spaces have been used in the multiclass task, including color [18], shape [19] and texture features [17]. These features are commonly combined with classification methods (support vector machines-SVM, random forest, linear discriminant analysis-LDA) [5]. Currently deep learning strategies are the best to discriminate only leukemia cells in peripheral blood images with the ResNext [22], the VGG-Net [4] or customized networks [4]. A much more complicated task relies on the discrimination of atypical cells which for peripheral blood samples has been tackled using a ResNext network (accuracy = 0.99) [22]. Likewise, they have been discriminated as part of a multiclass BM cell problem with more sub-types than the atypical ones, using the same ResNext architecture (accuracy = 0.90) [21], or the You Only Look Once (YOLO) [26]. Additionally, the emerging transformers have also being used to differentiate multiple cell sub-types in BM, particularly by using a CoAtNet [9] which integrates transformer-attention layers and ConvNet deep neural network architecture, and provides state-of-the-art performance (accuracy = 0.93) [27].

Unlike previous works, the presented approach is focused in quantifying changes in the most common pathological atypical BM cell subtypes, namely myelocytes (MYB), blasts (BLA), promyelocytes (PMO), and erythroblast (EBO), achieving a quantitative strategy to differentiate atypical BM cells regardless the disease they are associated with. Differentiating these classes is crucial since the proposed 4 cell subtypes are the ones which must be counted for a correct diagnosis and morphological characterization of acute myeloid leukemia and myelodysplasic disease [28], currently the most common and aggressive hematological disorders in adults. This classification task is so complex that even common immunohistochemical hematology stains like CD117 may also misclassify these cell sub-types [23]. The introduced methodology builds upon One-class

variational autoencoders (OCVAE) and presents a new atypical BM cell representation by concatenating the latent spaces provided by 4 specialized OCVAE with the same architecture. In contrast to previous OCVAE applications focused on one-class training for binary classification [15], or anomaly detection based on the reconstruction quality [29], the introduced methodology presents a cascade of OCVAEs as feature extractor in a 4 class differentiation task. The methodology setting process splits data into two disjoint subsets, where the first one is used to set the OCVAEs parameters for capturing the particular patterns of each cell sub-type, separately. The second subset feeds all the trained OCVAEs for building a concatenated latent-space that serves to train different classifiers (support vector machine-SVM with linear and RBF kernel, and random forest), reporting accuracy, precision, recall and f1-score, as performance metrics. This approach was evaluated on a subset ($n = 26,000$) of a public image database [20], demonstrating to outperform previously published strategies, while requiring a lower number of training images.

2 Materials and Methods

2.1 The BM Smear Image Dataset

All experiments in the presented work were performed using a subset of the public image database "*An Expert-Annotated Dataset of Bone Marrow Cytology in Hematologic Malignancies*" [20]. This database is composed of 171,374 single-cells annotated by type, coming from the BM smears of a group of 945 patients covering a set of diseases, yet the individual hematological disease is not informed. All images were acquired using bright-field microscope with $\times 40$ magnification and oil immersion, applied to May-Grünwald-Giemsa/Pappenheim stained samples. Each image was annotated by an expert morphologist at the Munich Leukemia Laboratory (MLL), assigning one out of 21 possible classes, including the atypical BM cells that the herein presented methodology is working with, i.e., myelocytes (MYB), blasts (BLA), promyelocytes (PMO), and erythroblast (EBO). Particularly, the subset herein used was composed of a balanced version of the aforementioned classes, making a new dataset of 26,000 images (6,500 for each of the four classes).

Data Use Declaration. The complete version of the public database used for validating the proposed strategy is provided by Matek et. al., under the TCIA Data Usage Policy and Restrictions, and it is publicly available at TCIA platform, https://doi.org/10.7937/TCIA.AXH3-T579. No ethical compliance statement is presented in this document since it is covered by the original dataset publication [20].

2.2 OCVAE Atypical BM Cell Differentiation Method

Single Cell Image Pre-processing. The first step of the presented approach is to apply a color-space transformation from RGB to Lab, for reducing possible

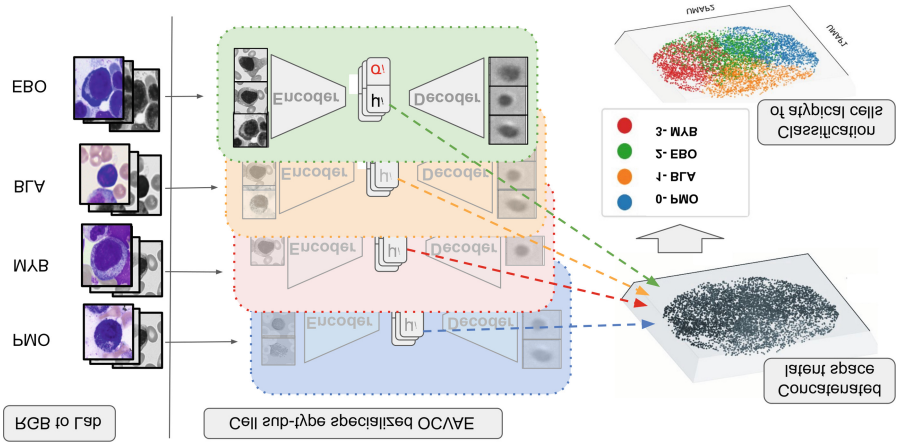

Fig. 1. Atypical BM cell characterization methodology: single cell images are transformed from RGB to Lab color space, b-channel image versions feed specialized OCVAES, and a cascade of latent space parameters (means-μ and variances-σ) are used to train classical classifiers (Random forest, SVM-linear and RBF kernel) that differentiates the 4 proposed classes (PMO, EBO, BLA and MYB).

illumination and stain variability effects. In the Lab color representation, the luminance component is isolated in the *L-channel*, and the remaining components (a and b) are more robust to the mentioned sources of variability [31]. Particularly, for the herein introduced work, only the *b-channel* is used to represent the whole set of images, taking into account that non-white blood cell image elements and background are homogenized in this particular Lab component.

Atypical BM Cell OCVAE Latent Space Representation. The main part of the introduced atypical BM cell characterization is based on a latent space representation of a variational autoencoder (VAE) bottleneck [16]. As commonly found in autoencoder strategies, the VAE encodes input data x by forcing dimensionality reduction to a bottleneck (latent space z) and decodes the compressed signal ($\hat{x} = f_{decoding}(z)$), aiming to minimize the output reconstruction error $\mathcal{L}_{rec} = |x - \hat{x}|_2^2$. The latent space is described by a set of parameterized distributions (mean-μ and variance-σ), and imposes these distributions to be as close as possible to unitary Gaussians. This guarantees a continuous approximation of the latent space by the Parzen theorem, i.e. $z \sim \mathcal{N}(0, 1)$, in terms of the Kullback-Leibler divergence (KLD) between the parametric posterior and the true posterior distributions.

Furthermore, to enhance VAE cell description, the presented approach takes advantage of the dedicated one-class characterization to force inter-class separability but increasing intra-class proximity. One-class classification strategies have been mainly used to find outlier samples in a given data space [6,24], with successful application in image related tasks [29], even using the reconstruction error

of variational autoencoders (VAE) [14]. As shown in Fig. 1, unlike previously published strategies that are mainly set to identify anomalies or fake samples by using the autoencoder reconstruction error in a binary task [2], the presented strategy uses the regularized representation of a VAE bottleneck, without using the reconstruction quality, but the latent space ability to separate the proposed classes. The presented strategy trains a set of 4 specialized VAEs, each adjusted for estimating a representation of one atypical cell class (OCVAE). After that, all testing images pass through each specialized OCVAE (OCVAEs cascade), in a blind characterization process. Finally, all test encoded outputs, composed of means and variances, are concatenated in a single feature space which feeds different classifiers that discriminate image samples of the four atypical BM cell types. Additionally, the obtained feature matrix is normalized after concatenation, decreasing the bias possibility, given the separately trained OCVAEs.

In a more detailed description, the implemented VAE encoder is composed of 3 convolutional and 2 max-pooling, intercalated layers, followed by a flatten, a fully connected, and a lambda layer which is customized for sampling the latent space in terms of means μ and variances σ. Here the bottleneck is set to compress the input layer dimension ($256 \times 256 \times 1$) in terms of 64 Gaussian distributions, i.e., $\mu_{i:\{1-64\}}$ and $\sigma_{i:\{1-64\}}$. The decoder architecture follows similar encoder's layer organization (3 convolutional and 3 up-sampling layers), but returning the original dimensionality to the reconstructed images.

Evaluation. The introduced concatenated OCVAE representation is quantitatively evaluated by classifying the four proposed classes (PMO, BLA, MYB, EBO). The OCVAE cascade training is carried out by using 80% of the dataset ($n = 20,800$), i.e., parameters of each specialized OCVAE model are found by using $5,200$ images coming from each of the proposed classes. The remaining 20% of the dataset ($n = 5,200$), composed of equal number of cells per class ($n = 1,300$), is used to obtain the feature space for evaluating the presented methodology while assuring independence to the parameterization image set. This independent data partition feeds the previously obtained specialized OCVAE encoder models, and the bottleneck values are concatenated to build an atypical BM cell representation. Afterward, the feature concatenation is used to train three different classifiers (SVM with linear and RBF kernels, and Random Forest) for differentiating cell types that compose the sample space. This experiment uses five iterations of a five-fold cross validation over the obtained feature space (20% of images), for reducing possible batch effect. Mean accuracy, precision, recall and f1-score, with their correspondent standard deviations, are presented as performance metrics. Finally, the best classifier, selected based on the performance metrics, is optimized by using different OCVAE parameter combinations as inputs, i.e., latent-space distribution means together with the corresponding variances, only means or only variances.

A second experiment is done to provide a baseline comparison in classifying the 4 atypical cell classes, by using different strategies reported in the literature for this task, including classical handcrafted image features and deep neural

networks. For this evaluation procedure, classical image processing descriptors were included for providing a classification strategy that depends on both, the interpretability of the feature representation space and the classifier, like the one introduced in this work. This handcrafted representation comprises a set of 144 image features obtained from nucleus and cytoplasm as separated cell elements, and includes RGB-color space intensity statistics (mean, variance, kurtosis, skweness, entropy), Gray-level-Co-occurrence matrix statistics (contrast, dissimilarity, homogeneity, energy, correlation, angular second moment, Minkowski-Bouligand dimension), and shape descriptors (convexity, compactness, elongation, eccentricity, roundness, solidity, area, perimeter). All these features were used to train different classifiers from which an SVM classifier (linear kernel) provides the best performance with the proposed setup. Regarding deep learning approximations, different architectures were used, including two bench marking options Xception [8], ResNet50 [12], the network with the best published results on a related task based on attention-integrated network CoAtnet [9], and the ResNext [30] which was proposed by the database authors [21]. Furthermore, Xception and ResNet50 networks were trained by using imagenet weights along 30 epochs, while ResNext [21] and CoAtnet [27] evaluation uses the weights provided by the corresponding authors. Regarding the experimental setup, this comparison experiment follows the same data organization as presented in the first experiment, i.e., using 80% and 20% of the data, for training and testing respectively.

3 Results and Discussion

The results of the first experiment are shown in Table 1, where the overall classification performance of this multi-class problem demonstrates the best discrimination results were achieved with a SVM classifier (linear kernel), i.e., mean accuracy and recall of 0.881. Interestingly, regardless the implemented classifier, all the obtained performance values are higher than 0.86, indicating that differentiation stability relies on the concatenated OCVAE characterization space. In addition, as presented in Table 2, the OCVAE SVM-linear kernel results can be optimized by feeding the classifier only with the OCVAE latent variances, leading to an improvement of almost 0.06 in all metrics (accuracy = 0.938, precision = 0.935, recall = 0.935, f1-score = 0.932), when comparing the same classifier but using the whole latent space (means and variances). Finally, Fig. 2 presents the results per-class by evaluating the SVM classifier with a linear-kernel, using only variances. Such results evidenced model stability regardless the atypical cell class, with all metrics going above 0.93.

Finally, the baseline experiment results, presented in the table 2, demonstrates the performance achieved by ResNet50 (accuracy = 0.624, precision = 0.24, recall = 0.25 and f1-score = 0.248) and Xception network (accuracy = 0.708, precision = 0.697, recall = 0.899, f1-score = 0.72) are lower than the obtained with the proposed strategy. In contrast, handcrafted features (accuracy = 0.843, precision = 0.688, recall = 0.684, f1-score = 0.685) ResNext network (accuracy = 0.79, precision = 0.78, recall = 0.74, f1-score = 0.72), and

Table 1. Overall classification results in differentiating 4 atypical BM cell classes by using the whole OCVAE latent space representation with 3 classifiers: SVM (linear/RBF kernels) and Random forest.

	Mean Accuracy (std)	Mean Precision (std)	Mean Recall (std)	Mean f1-score (std)
SVM linear kernel	**0.881 (0.006)**	**0.882 (0.005)**	**0.881 (0.006)**	**0.882 (0.005)**
SVM RBF	0.866 (0.008)	0.863 (0.008)	0.866 (0.007)	0.863 (0.008)
Random forest	0.879 (0.011)	0.879 (0.01)	0.88 (0.013)	0.878 (0.013)

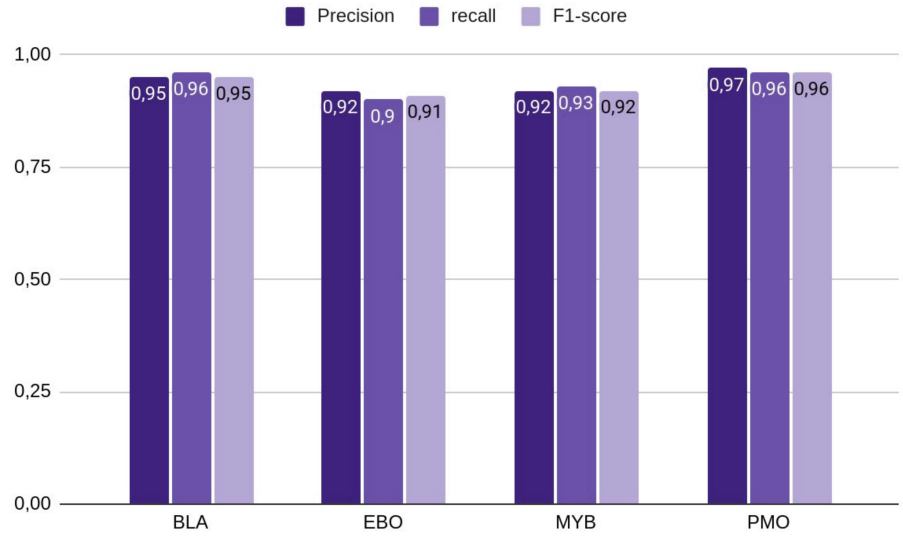

Fig. 2. Per class classification performance metrics (Precision, recall, F1-score), by using the concatenation of OCVAEs' variances as input of a SVM with a linear kernel.

CoAtnet (accuracy = 0.908, precision= 0.930, recall = 0.933, f1-score = 0.931) show better results among tested baseline methodologies, but still outperformed by optimized OCVAE cascade. Interestingly, the results of the bench marking networks are outperformed by the handcrafted-feature-based approach. These results are caused by the low number of training images, and the transference of learned weights from imagenet natural images, rather than cell related ones. Even where parameter optimization is applied to such networks, overfitting and 4 class complexity is affecting the predicting power of these architectures. Meanwhile, classical SVM take advantage of the separability given by pre-extracted features, which simplify the separation task and limits the overfitting risk. State-of-the-art networks, CoAtnet and ResNext, show better results by using images coming from the here in used database, instead of pre-trained network weights. Even when CoAtnet performance is closer to the introduced OCVAE cascade, it is important to highlight the low training data requirement of this approach ($n = 20,800$ for setting OCVAE feature extractor and $n = 5,200$ for training and testing the classifiers), compared to the amount of data used to train the

Table 2. Top panel: overall classification results by using different parameter combination for the introduced OCVAE (mean+variances, only means, only variances) and a SVM (linear kernel) to discriminate the 4 atypical BM cell types, showing the best performance results (blue) were obtained using just the variances of the OCVAE bottleneck. Bottom panel: the performance metrics of baseline methodologies including a classical image processing feature representation and 4 different deep learning architectures.

	Strategy	Accuracy	Precision	Recall	F1-score
Introduced OCVAE Parameter optimization	Variances and means	0.881	0.882	0.881	0.882
	Only Means	0.917	0.925	0.924	0.925
	Only Variances	**0.938**	**0.935**	**0.935**	**0.932**
Baseline comparison	Handcrafted image features	0.843	0.688	0.684	0.685
	ResNet50	0.624	0.24	0.25	0.248
	Xception	0.624	0.647	0.648	0.637
	ResNext	0.79	0.78	0.74	0.72
	CoAtnet	0.908	0.930	0.933	0.931

transformer-integrated network (CoAtnet- 20,000 images per class), according to the corresponding authors report [27]. Furthermore, the presented approach is computationally simpler and has a smaller risk of overfitting, a frequently reported problem when using data augmentation that may affect model generalization. This may be particularly true with myelocytes class since the set of 6,557 images is converted into 20,000. Finally, the mean accuracy improvement (3%), with respect to the state of the art (OCVAE_acc= 0.938, Coatnet_acc= 0.908), is fair enough for comparison purposes, given the low standard deviation of the proposed approach (acc_std= 0.006, f1_std= 0.006, prec_std= 0.0058).

Besides the classification performance, it is important to highlight that these results are obtained by the OCVAE bottleneck regularization, which reduces variance inflation and maximises the compactness of the feature space [15]. The previously mentioned OCVAE advantages, and the generative properties of this regularized latent-space prevent overfitting, but also as suggested by the results, provide a representation that keeps closer similar image concepts (cells that share similar patterns).

4 Conclusions

This work presents an atypical BM cell characterization strategy, which uses a concatenation of OCVAE's bottleneck parameters as a cell representation space. The combination of this space and an SVM classifier, demonstrates to successfully discriminate the 4 most common atypical cell types (PMO, BLA, MYO, EBO), while outperforms previously published strategies, with lower requirement of training images. This approach provides a tool for identifying these cell classes regardless the disease they are coming from, increasing the possibility of aiding differential blood counting in the presence of pathological conditions. Future work includes an independent evaluation by using other public databases and a more exhaustive baseline experimentation.

Acknowledgments. This work was supported in part by the project with code 110192092354 and entitle "Program for the Early Detection of Premalignant Lesions and Gastric Cancer in urban, rural and dispersed areas in the Department of Nariño" of call No. 920 of 2022 of MinCiencias.

References

1. Alférez, S., et al.: Automatic recognition of atypical lymphoid cells from peripheral blood by digital image analysis. Am. J. Clin. Pathol. **143**(2), 168–176 (2015)
2. An, J., Cho, S.: Variational autoencoder based anomaly detection using reconstruction probability. Spec. Lect. IE **2**(1), 1–18 (2015)
3. Anilkumar, K., Manoj, V., Sagi, T.: A survey on image segmentation of blood and bone marrow smear images with emphasis to automated detection of leukemia. Biocybernet. Biomed. Eng. **40**(4), 1406–1420 (2020)
4. Boldú, L., et al.: A deep learning model (ALNET) for the diagnosis of acute leukaemia lineage using peripheral blood cell images. Comput. Methods Prog. Biomed. **202**, 105999 (2021)
5. Boldú, L., et al.: Automatic recognition of different types of acute leukaemia in peripheral blood by image analysis. J. Clin. Pathol. **72**(11), 755–761 (2019)
6. Chalapathy, R., Menon, A.K., Chawla, S.: Anomaly detection using one-class neural networks. arXiv preprint arXiv:1802.06360 (2018)
7. Chen, W., et al.: The population characteristics of the main leukocyte subsets and their association with chronic diseases in a community-dwelling population: a cross-sectional study. Primary Health Care Res. Developm. **22** (2021)
8. Chollet, F.: Xception: deep learning with depthwise separable convolutions. In: Proceedings of the IEEE Conference on Computer Vision and Pattern Recognition, pp. 1251–1258 (2017)
9. Dai, Z., et al.: Coatnet: marrying convolution and attention for all data sizes. Adv. Neural Inf. Process. Syst. **34**, 3965–3977 (2021)
10. Fuentes-Arderiu, X., Dot-Bach, D.: Measurement uncertainty in manual differential leukocyte counting. Clin. Chem. Lab. Med. **47**(1), 112–115 (2009)
11. Gutiérrez, G., et al.: Eqas for peripheral blood morphology in Spain: a 6-year experience. Int. J. Lab. Hematol. **30**(6), 460–466 (2008)
12. He, K.,et al.: Deep residual learning for image recognition. In: Proceedings of the IEEE Conference on Computer Vision and Pattern Recognition, pp. 770–778 (2016)
13. Hodes, A., et al.: The challenging task of enumerating blasts in the bone marrow. In: Seminars in Hematology, vol. 56, pp. 58–64. Elsevier (2019)
14. Khalid, H., Woo, S.S.: Oc-fakedect: classifying deepfakes using one-class variational autoencoder. In: Proceedings of the IEEE/CVF Conference on Computer Vision and Pattern Recognition Workshops, pp. 656–657 (2020)
15. Kim, B., Ryu, K.H., Kim, J.H., Heo, S.: Feature variance regularization method for autoencoder-based one-class classification. Comput. Chem. Eng. **161**, 107776 (2022)
16. Kingma, D.P., Welling, M.: Auto-encoding variational bayes. arXiv preprint arXiv:1312.6114 (2013)
17. Krappe, S., et al.: Automated classification of bone marrow cells in microscopic images for diagnosis of leukemia: a comparison of two classification schemes with respect to the segmentation quality. In: SPIE Proceedings. SPIE (2015). https://doi.org/10.1117/12.2081946

18. Krappe, S., et al.: Automated morphological analysis of bone marrow cells in microscopic images for diagnosis of leukemia: nucleus-plasma separation and cell classification using a hierarchical tree model of hematopoesis. In: Medical Imaging 2016: Computer-Aided Diagnosis. SPIE (2016). https://doi.org/10.1117/12.2216037
19. Liu, H., Cao, H., Song, E.: Bone marrow cells detection: a technique for the microscopic image analysis. J. Med. Syst. **43**(4), 1–14 (2019)
20. Matek, C., et al.: An expert-annotated dataset of bone marrow cytology in hematologic malignancies (2021). https://doi.org/10.7937/TCIA.AXH3-T579, https://wiki.cancerimagingarchive.net/x/CoITBg https://wiki.cancerimagingarchive.net/x/CoITBg
21. Matek, C., et al.: Highly accurate differentiation of bone marrow cell morphologies using deep neural networks on a large image data set. Blood J. Am. Soc. Hematol. **138**(20), 1917–1927 (2021)
22. Matek, C., et al.: Human-level recognition of blast cells in acute myeloid leukemia with convolutional neural networks (2019). https://doi.org/10.1101/564039
23. Nedumannil, R., Sim, S., Westerman, D., Juneja, S.: Identification and quantitation of blasts in myeloid malignancies with marrow fibrosis or marrow hypoplasia and cd34 negativity. Pathology **53**(6), 795–798 (2021)
24. Ruff, L., et al.: Deep one-class classification. In: International Conference on Machine Learning, pp. 4393–4402. PMLR (2018)
25. Shah, A., et al.: Automated diagnosis of leukemia: a comprehensive review. IEEE Access **9**, 132097–132124 (2021)
26. Tayebi, R.M., et al.: Automated bone marrow cytology using deep learning to generate a histogram of cell types. Commun. Med. **2**(1), 45 (2022)
27. Tripathi, S., et al.: Hematonet: expert level classification of bone marrow cytology morphology in hematological malignancy with deep learning. Artif. Intell. Life Sci. **2**, 100043 (2022)
28. Vanna, R., et al.: Label-free imaging and identification of typical cells of acute myeloid leukaemia and myelodysplastic syndrome by Raman microspectroscopy. Analyst **140**(4), 1054–1064 (2015)
29. Wei, Q., et al.: Anomaly detection for medical images based on a one-class classification. In: Medical Imaging 2018: Computer-Aided Diagnosis, vol. 10575, pp. 375–380. SPIE (2018)
30. Xie, S., et al.: Aggregated residual transformations for deep neural networks. In: Proceedings of the IEEE Conference on Computer Vision and Pattern Recognition, pp. 1492–1500 (2017)
31. Zhang, C., et al.: White blood cell segmentation by color-space-based k-means clustering. Sensors **14**(9), 16128–16147 (2014)
32. Zini, G., Bain, B., Castoldi, G.: Others: European leukemianet (ELN) project diagnostic platform (wp10): final results of the first study of the european morphology consensus panel. Blood **112**(11), 1645 (2008)